Rapid Communications

Formation of inverse electron distribution function and absolute negative conductivity in nonlocal plasma of a dc glow discharge

Chengxun Yuan,[1] Jingfeng Yao,[1] E. A. Bogdanov,[1,2,*] A. A. Kudryavtsev,[1,2] and Zhongxiang Zhou[1,†]
[1]*Department of Physics, Harbin Institute of Technology, Harbin 150001, China*
[2]*Faculty of Physics, St. Petersburg State University, 198504 St. Petersburg, Russia*

(Received 23 October 2019; accepted 6 March 2020; published 23 March 2020)

The inversion of the electron energy distribution function (EEDF) at low energies and the absolute negative electron conductivity are predicted and confirmed by numerical modeling of a direct current glow discharge in argon. It is shown that, in contrast to the local approximation used earlier for searching the inverse EEDF, in a real gas-discharge plasma, the formation of the EEDF is significantly affected by the terms with spatial gradients in the Boltzmann kinetic equation. In analogy with the inverse population of excited states in lasers, such a medium will amplify electromagnetic waves.

DOI: 10.1103/PhysRevE.101.031202

I. INTRODUCTION

The creation of nonequilibrium gas media with an inverse distribution of particles over energy states is of great interest to science and applications because these substances can be used as signal amplifiers. Thus, the prediction and implementation of inverse populations of the excited states of atoms and molecules make it possible in practice to create an extensive class of various lasers. In turn, plasma with an inverse distribution function of free electrons [electron energy distribution function (EEDF)] also has unique properties such as absolute negative conductivity (ANC) and the ability to amplify electromagnetic waves [1].

One of the first studies in which the conditions for negative conductivity in plasmas were formulated was conducted by Bekefi *et al.* [1]. The analysis of the expression of electron conductivity indicated that two conditions had to be satisfied to achieve negative conductivity: the presence of an inverse EEDF ($\partial f_0/\partial w > 0$) in a given energy range and a fairly sharp increase in the electron momentum transfer cross section σ_m with increasing energy [$d \ln \sigma_m(w)/d \ln w > 1$). The last condition is satisfied for heavy rare gases in the energy range just above the Ramsauer minimum.

In order to achieve the first basic condition, various attempts have been made since the 1960s–1970s [2–8]. Nevertheless, the results of recent studies are still not convincing. There is no also satisfactory experimental evidence for both the inverse EEDF and stationary ANC. In our opinion, the main reason for this ambiguous situation in the literature is the fact that searches for ANC were usually conducted on the basis of a local approximation, in which all terms with all spatial gradients are neglected in the Boltzmann kinetic equation and it depends on only the kinetic energy of electrons.

In the local approximation, the creation of an inverse EEDF is reduced to searching for a set of plasma-chemical processes, which selectively deplete the EEDF at low energies [3–6]. However, it seems an extremely difficult task because the collisional processes that can provide the sink at low energies inevitably increase the momentum transfer cross section σ_m and it leads to jamming of electrons and correspondingly to an increase in the EEDF. As a result, it is practically impossible to obtain the inversion of the EEDF under stationary conditions.

On the other hand, in real laboratory plasma objects the role of spatial gradients in the EEDF formation can be significant [9,10]. In this case, the EEDF is nonlocal and is described by the spatially inhomogeneous kinetic equation. A self-consistent electric field, which is the sum of the external electric field and the polarization field created by the plasma itself, plays the key role in the formation of a nonlocal EEDF. The presence of a polarization field leads to stratification of the plasma into wall layers of the space charge with a strong electric field and a quasineutral plasma with a weak ambipolar field [11]. The ambipolar field is determined by the EEDF and this makes the kinetic equation nonlinear. On the one hand, this significantly complicates the procedure for solving the Boltzmann kinetic equation. On the other hand, an increase in the number of degrees of freedom of the system leads to the appearance of fundamentally new scenarios of the EEDF formation. In particular, the divergence of the spatial flux is a source (or sink), which can provide inversion of the EEDF and, as a consequence, the formation of stationary ANC.

In this work, self-consistent kinetic modeling of gas-discharge plasma in argon is performed for the purpose of investigating the inversion of the EEDF and ANC.

II. THEORY

In the two-term approximation, in the absence of a magnetic field, the kinetic equation for the isotropic component f_0 of EEDF has the form [12–14]

$$w^{1/2}\frac{\partial f_0}{\partial t} + \nabla \cdot \mathbf{\Phi} + \frac{\partial \Gamma}{\partial w} = S(f_0), \tag{1}$$

$$\mathbf{\Phi} = \frac{\gamma}{3} w\, \mathbf{f}_1, \quad \Gamma = \frac{\gamma}{3} w \mathbf{E}\cdot\mathbf{f_1} - \left(\sum_k D_k\right)\frac{\partial f_0}{\partial w} - \left(\sum_k V_k\right) f_0, \tag{2}$$

*eugene72@mail.ru
†zhouzx@hit.edu.cn

where $\mathbf{f}_1 = -\lambda(\nabla f_0 - \mathbf{E}\,\partial f_0/\partial w)$, w is the electron kinetic energy in eV units, e is the elementary charge, m is the electron mass, $\mathbf{E}$ is the electric field vector, λ is the electron mean free path, $\gamma = (2e/m)^{1/2}$, $S(f_0)$ is the integral of inelastic collisions, and $\mathbf{\Phi}$ and Γ are the spatial and energy phase fluxes. The notation $S(f_0)$ indicates that S is determined by the isotropic part of the EEDF. $S = \sum_k S_k$ for various types of inelastic collisions. The coefficients D_k and V_k in Eq. (2) are the energy diffusion coefficient and the friction force for collision operators that can be represented in the Fokker-Planck form. The collision terms S_k for various types of inelastic collisions and coefficients D_k, V_k for the elastic and Coulomb collisions can be found in many textbooks and reviews [12,14–16].

From the foregoing, it is clear that in order to create ANC, it is necessary to create an inversion of the EEDF at low energies. Further, to analyze the behavior of the EEDF at low energies, we find the limiting value of the kinetic equation (1) at $w \to 0$. Under the natural assumption that both f_0 and its partial derivatives are continuous at $w = 0$, all the terms in Eq. (1), except $\partial\Gamma/\partial w$, vanish at $w \to 0$. Further, the contributions in $\partial\Gamma/\partial w$ from the elastic and Coulomb collisions also disappear since $D_{\rm el}\partial f_0/\partial w + V_{\rm el} f_0 = O(w^2)$ and $D_C\partial f_0/\partial w + V_C f_0 = O(w^{3/2})$ when $w \to 0$ (in reality, to obtain these results, it is necessary to make several rather trivial additional assumptions, namely, that $d\sigma_0/dw$ and $d\lambda/dw$ are limited and the cross sections of the inelastic processes are continuous at the energy threshold $w = \varepsilon_k$). For the remaining term, we have $\partial(w\,\mathbf{E}\cdot\mathbf{f}_1)/\partial w = \mathbf{E}\cdot\mathbf{f}_1 + w\,\partial(\mathbf{E}\cdot\mathbf{f}_1)/\partial w \to \mathbf{E}\cdot\mathbf{f}_1$ at $w \to 0$. But then $\mathbf{E}\cdot\mathbf{f}_1|_{w=0} = 0$ and the division by $\lambda(0)$ provides

$$\left(\mathbf{E}\cdot\nabla f_0 - E^2\frac{\partial f_0}{\partial w}\right)\Bigg|_{w=0} = 0. \tag{3}$$

It should be noted that Eq. (3) is not a boundary condition but a consequence of the kinetic equation. On the $w = 0$ surface, the condition $\Gamma(0) = 0$ is satisfied for any smooth f_0 and it is impossible to set any additional constraints. This occurs because the surface $w = 0$ is not a real boundary but a singular point of the spherical coordinates system in the space of velocities.

It follows from Eq. (3) that if f_0 increases in the direction of the electric field, then, and consequently, $(\partial f_0/\partial w)|_{w=0} > 0$. That is, the EEDF has an inversion in the vicinity of zero energy. In the case when the discharge geometry is one dimensional, Eq. (3) becomes simpler. In this case $\mathbf{E} = E_x\mathbf{e}_x$, $\nabla f_0 = (\partial f_0/\partial x)\mathbf{e}_x$, where $\mathbf{e}_x$ is a unit vector in the direction of the axis and, therefore, at $E \neq 0$ we have

$$(\partial f_0/\partial w)|_{w=0} = (\partial f_0/\partial x)|_{w=0}/E_x. \tag{4}$$

It follows from Eq. (4) that if the electric field at some point x_0 changes sign, then $(\partial f_0/\partial w)|_{w=0}$ changes sign if and only if $(\partial f_0/\partial x)|_{w=0}$ does not change sign. If the field does not change sign at $x = x_0$, then $(\partial f_0/\partial x)|_{w=0}$ and $(\partial f_0/\partial w)|_{w=0}$ change or do not change sign, but only together. If $(\partial f_0/\partial x)|_{w=0} < 0$ and $E_x < 0$ (which corresponds to an increase in potential), then $(\partial f_0/\partial w)|_{w=0} > 0$, that is, f_0 has an inversion at $w = 0$. In the form presented here, Eqs. (3) and (4) were obtained in our previous work [17].

In the two-term approximation, the total electron flux has the drift-diffusion form [14]

$$\mathbf{J}_e(\mathbf{x}) = \int_0^\infty \mathbf{\Phi}(\mathbf{x}, w)dw = -\nabla(D_e n_e) - \mu_e \mathbf{E} n_e, \tag{5}$$

where $n_e = \int_0^\infty f_0(w)w^{1/2}dw$ is the electron density, and D_e and μ_e are the electron diffusion coefficient and mobility:

$$D_e = (1/n_e)\int_0^\infty D_r f_0 w^{1/2}dw,$$
$$\mu_e = -(1/n_e)\int_0^\infty D_r\frac{\partial f_0}{\partial w}w^{1/2}dw, \tag{6}$$

where $D_r = v\lambda(w)/3$ is the diffusion coefficient. Electron mobility and conductivity are proportional: $\sigma_e = \mu_e n_e$. The electron temperature in the non-Maxwellian plasma is determined as 2/3 of the mean electron energy: $T_e = 2/(3n_e)\int_0^\infty f_0(w)w^{3/2}dw$.

It can be seen from Eq. (6) that the intervals at which $\partial f_0/\partial w > 0$ make a negative contribution to the electron conductivity and mobility, i.e., EEDF inversion is a necessary condition for negative conductivity and mobility. Next, we will analyze the conditions under which an inverse EEDF is possible in a dc glow discharge.

Recall that the longitudinal structure of a classical dc glow discharge is determined by the parameter pL [11,15,18–20], where L is the length of the discharge gap and p is the gas pressure. Numerous studies have found that the presence or absence of a positive column region depends on the pL value [11,18,19]. In short (without a positive column) discharges, the electrons in the negative glow region are trapped in the potential well and their density satisfies the Boltzmann distribution $n_e \sim \exp(\varphi/T_e)$. In this case $\mathbf{E} \approx -T_e\nabla \ln n_e$ and there is only one field reversal point $\mathbf{E} = 0$ at the maximum of the electron density. In this case the electric field attracts ions to the anode and the space charge in the anode layer is positive.

With an increase in the pL parameter, the positive column will form. Since the electric field in the positive column is negative (has the same sign as in cathode fall), then there must be at least two points of electric field reversal in the discharge with the positive column. At high pressures, the longitudinal structure of a glow dc discharge is exactly the same as that of the classical low-pressure discharge, but instead of the positive column with the diffusive losses of charged particles, an axially homogeneous plasma region with recombination losses appears [11,21]. This region can be called the recombination-dominated positive column [22].

Thus, if we begin from a short glow discharge and gradually increase the pL parameter (for example, by increasing the gas pressure p at fixed L), then we must obtain at some p a discharge with two points of electric field reversal x_1, x_2 : $0 < x_1 < x_2 < L$ (such transition was observed experimentally in [23]). Further, when approaching the anode, the electron density decreases at $x > x_2$, and $\partial n_e/\partial x < 0$. The EEDF at zero energy should qualitatively reproduce the electron density profile: $n_e(x) \sim f_0(x, w = 0)$. Therefore, when $x > x_2$ there should be a region where $(\partial f_0/\partial x)|_{w=0} < 0$ and $E_x < 0$. Then, based on Eq. (4), $(\partial f_0/\partial w)|_{w=0} > 0$, i.e., the EEDF has an inversion at zero energy.

This qualitative reasoning can easily be extended to the case when there is an even number of electric field reversals since in this case [20,23], the electric field and space charge on the anode are negative and after the last point of field reversal, we have $E_x < 0$ and $(\partial f_0/\partial x)|_{w=0} < 0$ and, therefore, $(\partial f_0/\partial w)|_{w=0} > 0$.

III. RESULTS AND DISCUSSION

To verify in detail the above analysis, we used numerical modeling with the solution of the spatially inhomogeneous kinetic equation for electrons. The one-dimensional kinetic model of a glow discharge that was developed in our previous work [17] in the COMSOL MULTIPHYSICS software environment was chosen as the basis. We modified this model to study discharges in helium and argon for $pL = 10$ cm Torr. Since [17] contains a detailed description of this model, we briefly describe here only changes made to the model for this study. A COMSOL model file is provided in the Supplemental Material [24].

The model includes the kinetic equation (1) for electrons, drift-diffusion fluid balance equations for heavy particles, and the Poisson equation. In order to exclude a large interval of kinetic energies of electrons in the cathode drop of a cold cathode (200–300 eV), we used a model of a heated cathode with a low value of the cathode potential drop ($U_0 = 50$ V) and a fixed emission current density J_e at the cathode.

As in [17], the plasma-chemical model included direct excitation, direct and stepwise ionizations, superelastic collisions of electrons with metastable atoms, and Penning ionization. At high pressures ($p = 20$ Torr), dissociative recombination should be taken into account in order to describe the annihilation of charges. (The cross section $\sigma_{\rm rec} = 5 \times 10^{-20}$ m^2 was used in the calculations [11,15].)

The numerical modeling results showed that in all our calculations with two or more points of electric field reversal, the EEDF has an inversion at $w = 0$ in some spatial intervals, which is in accordance with Eq. (4). It should be noted that the EEDF inversion cannot be observed in a positive column region that is ideally uniform in the longitudinal direction, since

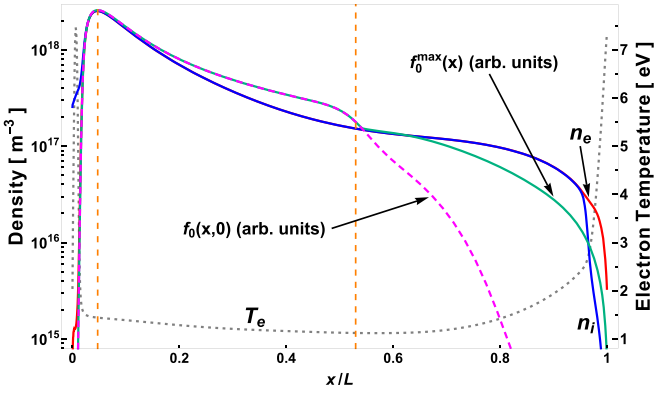

FIG. 1. The profiles of electron density n_e, ion density n_i, electron temperature T_e, $f_0(x, 0)$, and the maximal value of the EEDF at a given x, $f_0^{\max}(x)$. The vertical dashed lines show the points of electric field reversal.

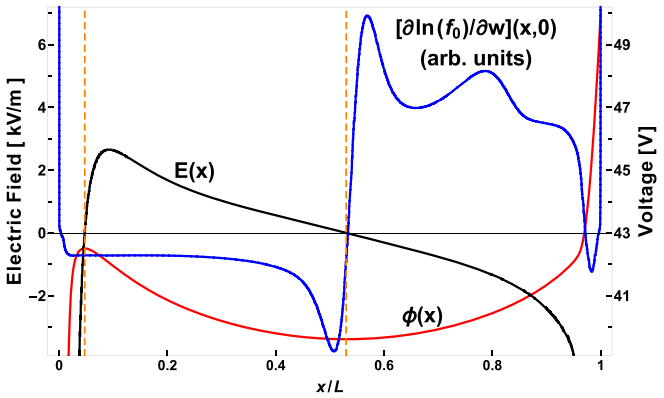

FIG. 2. The profiles of the electric potential $\varphi(x)$, electric field $E_x(x)$, and $(\partial f_0/\partial w)|_{w=0}$ (in arbitrary units) for the same discharge calculation as in Fig. 1. The vertical dashed lines show the points of electric field reversal.

in this case $E_x < 0$ and $\partial f_0/\partial x = 0$; therefore, according to Eq. (4), $(\partial f_0/\partial w)|_{w=0} = 0$.

Most interesting were the results for $p = 20$ Torr and $L = 5$ mm in argon, at such emission currents that there are two points of electric field reversal but a positive column has not yet formed. Figures 1–5 show the results of calculating the plasma and EEDF parameters for one such regime with an emission current density of $J_e = 7 \times 10^{20}$ m^{-2} s^{-1}. Figure 1 shows the electron and ion density profiles, the electron temperature profile, $f_0(x, 0)$, and the EEDF maximum for a given coordinate $f_0^{\max}(x)$. Figure 2 shows the profiles of the electric potential, the electric field, and the EEDF derivative $(\partial f_0/\partial w)|_{w=0}$.

Figure 1 indicates that up to the second field reversal ($x_2 = 0.53L$), the curves $f_0(x, 0)$ and $f_0^{\max}(x)$ coincide. However, $f_0(x, 0) < f_0^{\max}(x)$ when $x > x_2$. That is, when $x > x_2$ there is an inversion of the EEDF. The same is observed in Fig. 2, where the $(\partial f_0/\partial w)|_{w=0}$ profile is presented. At the first point of the field reversal $x = x_1$, $(\partial f_0/\partial w)|_{w=0}$ does not change sign.

It is observed in Fig. 2 that at the second point of field reversal x_2, $(\partial f_0/\partial w)$ $(x, w = 0)$ changes sign. After the second point of field reversal, there is a large plasma region where

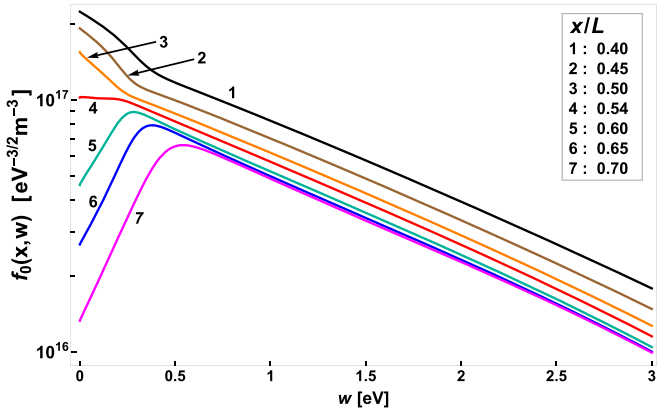

FIG. 3. $f_0(x, w)$ for different values of the coordinate x for the same discharge calculation as in Fig. 1.

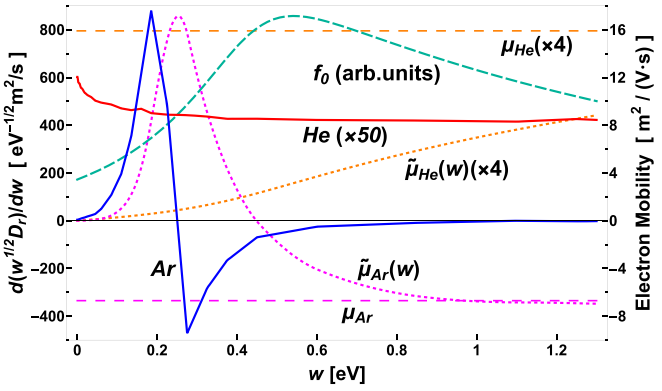

FIG. 4. The coefficients $d[w^{1/2}D_r(w)]/dw$ for argon and helium and the corresponding functions $\tilde{\mu}_{\rm Ar}(w)$ and $\tilde{\mu}_{\rm He}(w)$. The EEDF (dashed curve) is the same as in Figs. 1–3, for $x = 0.7\,L$. The dashed horizontal lines correspond to the electron mobilities $\mu_{Ar}$and μ_{He} in argon and helium, respectively calculated for this EEDF.

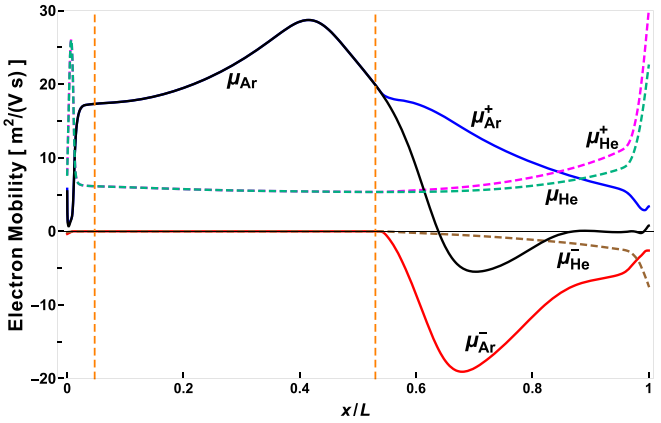

FIG. 5. The spatial profiles of the electron mobility in argon $\mu_{\rm Ar}$ and its positive $\mu^+_{\rm Ar}$ and negative $\mu^-_{\rm Ar}$ components calculated for the same EEDF as in Figs. 1–4. For comparison, the dashed lines show the profiles of $\mu_{\rm He}$, $\mu^+_{\rm He}$, and $\mu^-_{\rm He}$ calculated for the same EEDF but with a cross section of helium. The vertical dashed lines show the points of electric field reversal.

$(\partial f_0/\partial w)|_{w=0} > 0$. Figure 2 also shows that $(\partial f_0/\partial w)|_{w=0}$ changes sign at two additional points at a nonzero electric field.

Figure 3 shows the EEDF for different coordinate values. It is observed that EEDF has the inversion at $w = 0$ when $x > x_2$. In our calculations, we obtained $\mu_e < 0$ for the inverse EEDF in argon but not in helium. This is due to the special nature of the transport cross section in argon (and other rare gases, except for helium and neon). It is well known that the elastic cross section of argon has the so-called Ramsauer minimum, which is the energy region near $w = 0.1$ eV where the cross section is very small. To understand how negative mobility is related to the behavior of the cross section, it is useful to rewrite Eq. (6) for electron mobility in a different form using integration by parts and taking into account that $f_0(w)$ rapidly decreases at $w \to \infty$:

$$\mu_e = (1/n_e)\int_0^\infty f_0 \frac{d}{dw}(D_r w^{1/2})dw. \qquad (7)$$

It is clear from Eq. (7) that in order to obtain $\mu_e < 0$, the coefficient $w^{1/2}D_r$ must decrease with w over a certain energy range. Since $w^{1/2}D_r = \gamma\, w/(3N_0\sigma_m)$ (where N_0 is the gas density), it is necessary that the cross section $\sigma_m(w)$ grows sharply in a certain energy range. Since $\int_0^{w_1} \partial(w^{1/2}D_r)/\partial w\, dw = w_1 D_r(w_1) > 0$, in order to obtain a negative value of μ_e, it is necessary that negative values of $d(w^{1/2}D_r)/dw$ in the integral in Eq. (7) have a larger weight than the positive values. That is, the maximum of f_0 should be located in the area where $d(w^{1/2}D_r)/dw < 0$. This is illustrated in Fig. 4, which shows the $d[w^{1/2}D_r(w)]/dw$ coefficients for argon and helium. The figure also shows the functions $\tilde{\mu}_{Ar}(w)$ and $\tilde{\mu}_{\rm He}(w)$, which are the results of the replacement of the infinite upper limit in the integral in Eq. (7) with w calculated for the same EEDF.

It is seen that for helium, the coefficient $d[w^{1/2}D_r(w)]/dw > 0$ at all energies, whereas it is alternating for argon. It is also observed that the maximum of f_0 is in the region where $d(w^{1/2}D_r)/dw < 0$; this makes the integral in Eq. (7) negative.

Figure 5 shows the profile of the electron mobility $\mu_{\rm Ar}$ in argon and the positive and negative components $\mu^+_{\rm Ar}$ and $\mu^-_{\rm Ar}$ calculated for the same EEDF as in Figs. 1–4. The positive and negative components here are the values calculated by Eq. (6) and not over the entire energy range $(0; +\infty)$ but over those intervals where $\partial f_0/\partial w$ is positive or negative, respectively. For comparison, the profiles of $\mu_{\rm He}$, $\mu^+_{\rm He}$, and $\mu^-_{\rm He}$ are presented. It is observed that negative contributions are present for both argon and helium but the mobility is negative only for argon, which is in accordance with Eq. (7) (and Fig. 5) and in a much narrower interval $(0.65L \leqslant x \leqslant 0.85L)$ than the inversion region $(x < x_2 = 0.53L)$.

IV. CONCLUSION

Self-consistent kinetic modeling of gas-discharge plasma in argon was performed to investigate the inversion of the EEDF and obtain the ANC. It is shown that, in laboratory plasma, the formation of the EEDF is significantly affected by the terms with spatial gradients in the Boltzmann kinetic equation. In particular, it is shown that the divergence of the spatial flux $\nabla \cdot \mathbf{\Phi}$ is a sink in some plasma regions, which ensures inversion of the EEDF at low energies and, as a result, the formation of a stationary ANC in the rare gases with Ramsauer minimum. Since the imaginary part of the plasma dielectric constant is proportional to the conductivity [25], a plasma with negative conductivity should amplify electromagnetic waves.

[1] G. Bekefi, J. L. Hirshfield, and S. C. Brown, Phys. Fluids **4**, 173 (1961).

[2] Z. L. Petrovic, R. W. Crompton, and G. N. Haddad, Aust. J. Phys. **37**, 23 (1984).

[3] R. E. Robson, Z. L. Petrovic, Z. M. Raspopovic, and D. Loffhagen, J. Chem. Phys. **119**, 11249 (2003).
[4] N. A. Dyatko, J. Phys.: Conf. Ser. **71**, 012005 (2007).
[5] N. A. Dyatko, D. Loffhagen, A. P. Napartovich, and R. Winkler, Plasma Chem. Plasma Process. **21**, 421 (2001).
[6] N. A. Dyatko, A. P. Napartovich, S. Sakadzic, Z. Petrovic, and Z. Raspopovic, J. Phys. D: Appl. Phys. **33**, 375 (2000).
[7] J. M. Warman, U. Sowada, and M. P. De Haas, Phys. Rev. A **31**, 1974(R) (1985).
[8] Z. Donko and N. Dyatko, Eur. Phys. J. D **70**, 135 (2016).
[9] K. D. Kapustin, A. A. Kudryavtsev, and M. V. Krasilnikov, Phys. Plasmas **21**, 120701 (2014).
[10] C. Yuan, E. A. Bogdanov, A. A. Kudryavtsev, K. M. Rabadanov, and Z. Zhou, Sci. Rep. **7**, 14613 (2017).
[11] Yu. P. Raizer, *Gas Disharge Physics* (Springer-Verlag, Berlin/Heidelberg, 1991), p. 449.
[12] I. P. Shkarofsky, T. W. Johnston, and M. P. Bachynski, *The Particle Kinetics of Plasmas*, 1st ed. (Addison Wesley, Reading, MA, 1966), p. 518.
[13] T. W. Johnston, Phys. Rev. **120**, 1103 (1960).
[14] U. Kortshagen, C. Busch, and L. D. Tsendin, Plasma Sources Sci. Technol. **5**, 1 (1996).
[15] M. A. Liebermann and A. J. Lichtenberg, *Principles of Plasma Discharges and Materials Processing*, 2nd ed. (Wiley, New York, 2005), p. 800.
[16] J. G. M. Hagelaar, Plasma Sources Sci. Technol. **25**, 015015 (2016).
[17] C. Yuan, E. A. Bogdanov, S. I. Eliseev, and A. A. Kudryavtsev, Phys. Plasmas **24**, 073507 (2017).
[18] V. I. Kolobov and L. D. Tsendin, Phys. Rev. A **46**, 7837 (1992).
[19] A. A. Kudryavtsev, A. V. Morin, and L. D. Tsendin, Tech. Phys. **53**, 1029 (2008).
[20] K. A. Barzilovich, E. A. Bogdanov, and A. A. Kudryavtsev, Tech. Phys. Lett. **40**, 581 (2014).
[21] M. Capitelli, C. M. Ferreira, B. F. Gordiets, and A. I. Osipov, *Plasma Kinetics in Atmospheric Gases* (Springer-Verlag, Berlin/Heidelberg, 2000), p. 300.
[22] R. N. Franklin and J. Snell, J. Phys. D: Appl. Phys. **27**, 2102 (1994).
[23] E. I. Prokhorova, A. A. Kudryavtsev, A. A. Platonov, and A. G. Slyshov, Tech. Phys. **62**, 1122 (2017).
[24] See Supplemental Material at http://link.aps.org/supplemental/10.1103/PhysRevE.101.031202 for the COMSOL model file.
[25] V. L. Ginsburg, *The Propagation of Electromagnetic Waves in Plasmas*, 2nd ed. (Pergamon, New York, 1970), p. 615.